J Geod
DOI 10.1007/s00190-011-0485-8

ORIGINAL ARTICLE

A global mean dynamic topography and ocean circulation estimation using a preliminary GOCE gravity model

P. Knudsen · R. Bingham · O. Andersen · Marie-Helene Rio

Received: 22 October 2010 / Accepted: 10 May 2011

Abstract The Gravity and steady-state Ocean Circulation Explorer (GOCE) satellite mission measures Earth's gravity field with an unprecedented accuracy at short spatial scales. In doing so, it promises to significantly advance our ability to determine the ocean's general circulation. In this study, an initial gravity model from GOCE, based on just 2 months of data, is combined with the recent DTU10MSS mean sea surface to construct a global mean dynamic topography (MDT) model. The GOCE MDT clearly displays the gross features of the ocean's steady-state circulation. More significantly, the improved gravity model provided by the GOCE mission has enhanced the resolution and sharpened the boundaries of those features compared with earlier satellite only solutions. Calculation of the geostrophic surface currents from the MDT reveals improvements for all of the ocean's major current systems. In the North Atlantic, the Gulf Stream is stronger and more clearly defined, as are the Labrador and the Greenland currents. Furthermore, the finer scale features, such as eddies, meanders and branches of the Gulf Stream and North Atlantic Current system are visible. Similar improvements are seen also in the North Pacific Ocean, where the Kuroshio and its extension are well represented. In the Southern hemisphere, both the Agulhas and the Brazil-Malvinas Confluence current systems are well defined, and in the Southern ocean the Antarctic Circumpolar Current appears enhanced. The results of this preliminary analysis, using an initial GOCE gravity model, clearly demonstrate the potential of the GOCE mission. Already, at this early stage of the mission, the resolution of the MDT has been improved and the estimated surface current speeds have been increased compared with a GRACE satellite-only MDT. Future GOCE gravity models are expected to build further upon this early success.

Keywords GOCE · Dynamic ocean topography · Ocean circulation · Altimetry

1 Introduction

As indicated by its name, a primary scientific goal of the GOCE mission is the determination of the ocean's steady state, or time mean circulation. Accurate measurement of this circulation is crucial if we are to fully understand ocean dynamics and the role the ocean plays in regulating the Earth's climate. The Gulf Stream and its extension, which transport heat poleward from the equator, helping to maintain the relatively temperate climate of western Europe (Rhines et al. 2008), and the East Greenland Current, which carries freshwater from the Arctic into the Atlantic, thereby ensuring the freshwater balance between the Atlantic and the Pacific (Woodgate et al. 1999), are but two examples.

Through geostrophy, the ocean's surface circulation is closely related to the ocean's mean dynamic topography (MDT), which is simply the mean height of the ocean's surface measured relative to the equi-potential gravitational surface known as the marine geoid. Through advances in satellite altimetry over the past several decades, the mean sea surface (MSS) is now known with centimetre accuracy. However, the ability to accurately measure the geoid has not progressed as

P. Knudsen (✉) · O. Andersen
Technical University of Denmark, DTU Space,
2100 Copenhagen, Denmark
e-mail: pk@space.dtu.dk

R. Bingham
School of Civil Engineering and Geosciences,
Newcastle University, Newcastle upon Tyne, UK

M.-H. Rio
CLS, Space Oceanography Division,
Ramonville-St-Agne, France

Published online: 19 June 2011

smoothly and has been the limiting factor in estimating the ocean's geostrophic circulation.

During the late 1980s, a sustained record of global satellite altimeter data was established. This prompted a concerted effort by the geodetic community to develop joint global geoid and MDT estimates, while at the same time reducing satellite orbit errors (Wagner 1986; Engelis and Knudsen 1989; Denker and Rapp 1990; Marsh et al. 1990; Nerem et al. 1990). Although the quality of the available data were not sufficient to recover the finer details of the ocean's general circulation, the largest scales (>5,000 km) of the ocean's MDT could be determined and compared with early oceanographic MDT estimates based on hydrographic data (e.g. Levitus and Boyer 1994). With such comparisons, consistency between reference ellipsoids and the impact of the permanent tidal correction on MDT calculations were identified as major issues. In parallel with these efforts, marine gravity data from ship-borne gravimeters was used to regionally improve the spatial resolution of the gravity field and geoid. By combining these locally enhanced geoids with altimeter data, more accurate and detailed estimates of the MDT were obtained (Wunsch and Zlotnicki 1984; Knudsen 1991, 1992).

More recently, the launches of the Gravity Recovery and Climate Experiment (GRACE) satellites in 2002 and ESA GOCE satellite in 2009 have delivered a large forward step in our ability to measure the Earth's gravity field. Together they are now providing a global picture of Earth's gravity and geoid with unprecedented accuracy and spatial resolution. In turn, the improved mapping of Earth's gravity in combination with satellite altimetry should allow the ocean's MDT to also be mapped from space with an accuracy and spatial resolution not previously obtained. This ability to accurately map the ocean's steady-state circulation from space should shed new light on the ocean's behaviour and will prove extremely useful in the drive to monitor and understand the Earth's changing climate (Johannessen et al. 2003).

In July 2010, the first GOCE gravity field models, based on 2 months (Nov–Dec 2009) of observations, were released to the scientific community. Three "flavours" of model were provided, produced by three distinct methods: the direct (DIR), the space-wise (SPW) and time-wise (TIM) methods, described in detail elsewhere in this issue. One important difference between the approaches is the degree to which a priori information is used to constrain the solution. On the one hand, the TIM model uses no a priori information. Arguably, therefore, it gives the most unambiguous demonstration of GOCE's capabilities. Recently, Bingham et al. (2011) have shown that the MDT and associated currents derived from the TIM solution for the North Atlantic basin represent a substantial improvement upon a similar MDT and current estimate from a state-of-the-art GRACE solution. Given that the latter is based on 8 years of observations, compared with just 2 months for the TIM solution, this is already a remarkable demonstration of the performance of GOCE.

On the other hand, at the opposite end of the scale, the DIR solution is constrained by the GRACE EIGEN5C gravity model, which in turn incorporates altimetry and other gravimetric surface data into its solution (Bruinsma et al. 2004). This blending of various observations permits higher-resolution (greater degree and order) solutions, albeit at the expense of transparency with regard to the source of these shorter-length scales. The DIR solution is defined to d/o 240, compared with d/o 224 for the TIM solution. This translates to potential MDT spatial resolutions, neglecting the impact of filtering, of approximately 83 and 89 km, respectively.

Initial investigations for the North Atlantic basin suggest that the additional constraints placed on the DIR solution does give an estimate of geostrophic surface currents that comes closer than the unconstrained solution to an independent estimate of the currents based solely on drifter data (Bingham et al. 2010). The reasons for this are twofold: First, the higher d/o means that the MDT slopes can potentially be better resolved. Second, the lower geoid commission error results in a less noisy MDT. Consequently, less filtering is required to remove this noise and so the MDT slopes are better preserved. For these reasons, we here focus on the DIR solution. This is combined with the new DTU10MSS to construct a global GOCE satellite-only MDT. The computation of the MDT follows the recommendations from the GOCE User Toolbox (GUT) tutorials and is carried out using GUT tools (Benveniste et al. 2007; the GUT toolbox together with the datasets required to calculate the MDTs described below can be downloaded from http://earth.esa.int/gut/).

The objective of this study is to provide an initial evaluation of GOCE's performance in terms of the MDT and associated geostrophic currents that, in combination with a MSS, can be estimated from it. Foremost is the question of whether the GOCE gravity model enables us to calculate a better MDT than could be achieved using a GRACE gravity model. In other words, has GOCE improved our ability to estimate the ocean's geostrophic circulation using the geodetic approach. To answer this question we use EIGEN-GL04S1 gravity model, produced using GRACE satellite data only (Förste et al. 2006). This gravity model is defined to d/o 150, corresponding to a minimum resolved spatial scale of about 130 km. The limited spectral, and therefore spatial, resolution of satellite geoid models means that ocean currents derived from them are generally weak in comparison with currents estimated from in-situ observations (e.g. Niiler et al. 2003), particularly for intense, narrow currents such as the Gulf Stream. Therefore, increased current speeds are in themselves a clear indication of an improved MDT estimate. This we find to be the case for the GOCE MDT in comparison with the estimate from GRACE.

However, to assess how good GOCE is in absolute terms, below we also evaluate the GOCE MDT against an MDT from Maximenko et al. (2009). This MDT is based on a combination of satellite and in-situ data. As such, the MDT owes its long wavelengths to a MSS minus GRACE geoid residual, and its shorter wavelengths to near-surface drifter data, filtered to remove inertial motions and corrected for Ekman drift. Hence, here it serves as "ground truth" for the shortest spatial scales in the GOCE-based geodetic MDT. This, of course, assumes that the currents provided by the drifter data are the "truth". If this is the case, then one may wonder why go to the trouble of trying to improve the resolution of the geodetic estimate. The reason, for now at least, is that it is reasonable to assume that, although not the truth, the currents obtained from the combined MDT come closer to the truth than can be presently be achieved by geodetic means. Moreover, it is worth striving to increase the resolution of the geodetic estimate because those scales that it can resolve will be more accurate than the same scales based on in-situ drifter data. This is because the in-situ estimate is not as direct as it at first seems due to the assumptions required to correct for non-geostrophic motions, inhomogeneous sampling in time and space and instrument problems.

The remainder of the paper is structured as follows: In Sect. 2 details of the procedure for estimating an MDT from a gravity model and mean sea surface are given. Although simple in theory, a number of complications arise in practice. Particular attention is paid to determining the degree of filtering that is required for each MDT, since this is fundamental to assessing the quality of the geodetic MDTs. The MSS used to calculate the geodetic MDTs is also described. In Sect. 3, the GOCE MDT is evaluated against a GRACE MDT and the Maximenko MDT. The analysis will focus on five regions of particular interest from oceanographic and climate perspectives: The North Atlantic region encompassing the Gulf Stream; The North Pacific region which includes the Kuroshio current and its extension; The Agulhas retroflection system off the Cape of Africa; The Brazil-Malvinas confluence in the South Atlantic; and finally the Antarctic Circumpolar Current (ACC) in the Southern Ocean. We show how GOCE improves the estimate of the MDT and associated geostrophic currents in each of these regions in comparison with the GRACE based estimate. Finally, in Sect. 4 we provide a concluding discussion.

2 Computation of the mean dynamic topography

The task of computing a mean dynamic topography (MDT) from a mean sea surface (MSS) and a geoid is conceptually very simple. Yet, there are some important practical issues that must be acknowledged in order to obtain a good MDT product. Most fundamentally, both the MSS and the geoid must be defined relative to the same reference ellipsoid and in the same tidal system. The MDT is then expressed by

$$\zeta = \bar{h} - N \tag{1}$$

where $\bar{h}$ is the height of the mean sea surface above the reference ellipsoid and N is the geoid height relative to the same reference ellipsoid. If the ultimate objective is to combine the MDT with altimetric sea level anomalies to obtain the ocean's absolute dynamic topography, then it is important to ensure that the MSS used in the MDT calculation and the sea level anomalies to be added to the time mean are consistent with regard to the time period to which they refer and with regard to the corrections that have been applied to the altimetric data in each case.

Another practical complication arises because the MDT is the small residual of two much large fields: Typical variations in the MSS and the geoid are up to 100 m, whereas for the MDT they are around 1m. Thus, even a one percent error in either the MSS or geoid can lead to an order of magnitude error in the MDT. It is generally accepted that the errors in the MSS are small relative to those in the geoid, so we now concentrate on the latter. The first type of geoid error that impacts on MDT calculations is omission error. This arises because global gravity field models such as the GOCE models are usually represented in terms of spherical harmonic coefficients up to a certain harmonic degree and order L. The value of L places a lower limit on the spatial scales captured by the gravity model of roughly 20,000/L km. Even with the GOCE DIR solution, for which L = 240 giving a shortest spatial scale of 83 km, the spatial resolution is much less than that of the MSS. Hence, when subtracting a geoid model based on such a set of coefficients from the MSS, the residual heights consist of the MDT plus the unmodelled parts of the geoid associated with harmonic degrees above L. Clearly, this MDT error decreases with increasing L.

In addition, the act of truncating the spherical harmonic model of the gravity model to obtain the geoid as a spatially gridded field leads to Gibbs type numerical artefacts in the gridded geoid that radiate away from strong gravity field gradients, produced by features such as mountain ranges on land and subduction trenches and sea mounts in the ocean. Although these errors are small in comparison with the magnitude of the geoid they can be significant in comparison with the magnitude of the MDT, and because they are non-local even features on land such as mountain ranges can lead to errors in the MDT (Hughes and Bingham 2008; Bingham et al. 2008). In other respects, this source of error shares the same characteristics and dependence on L as true physical omission error, and so the two can readily be grouped together under the umbrella of omission error.

Geoid commission error is the second form of geoid error that propagates in to the MDT estimate. Unlike the omission error, which results from the fact that spherical harmonic

terms are not defined above L, commission error is the error in the spherical harmonic terms that are defined. For a given gravity model, these tend to grow with increasing degree and order. Hence, while MDT errors due to geoid omission errors decrease with increasing L, the MDT errors due to the accumulated geoid commission error tend to increase with increasing L. Clearly then there is a trade off to be made in choosing the value of L, since a point will be reached where any decrease in omission error is offset by the increase in commission error.

Taking into account both geoid omission and commission error, we see that the estimated MDT is

$$\zeta' = \bar{h} - N_L = \zeta + N - N_L + \delta_L = \zeta + \Delta N_L + \delta_L \quad (2)$$

where ζ is the true MDT, ΔN_L is the geoid omission error (both physical and numerical) and δ_L is the geoid commission error. Both error terms in (2) produce small-scale noise in the calculated MDT, which must be removed to obtain a useful product. Because full error variance–covariance matrices are available for the GOCE gravity models, in the future it may be possible to construct a statistically optimal filter for the commission error component of the MDT noise. However, this is an area of on-going research. For now there are two possible approaches to removing the noise from an MDT. First, we can neglect any distinction between the two error sources and apply a spatial filter directly to the MDT. Alternatively, we can recognise the difference between the two errors by first applying a spectral filter to the MSS. By matching the spectral content of the geoid and MSS in this way we can almost eliminate the geoid omission error component of the error in (2). However, since the commission error component remains, it is still necessary to apply a spatial filter to the MDT. Bingham et al. (2008) found that spectrally filtering the MSS prior to computing the MDT did provide some advantages over spatial filtering of the MDT containing both components of the error budget. The approach may also be useful when more sophisticated forms of filtering, such as the anisotropic spatial filter used by Bingham et al. (2011) are employed. If optimal filters taking into account the GOCE error information can be developed, then eliminating the omission error beforehand should also be beneficial (e.g. Knudsen et al. 2007). Finally, by separating the omission and commission components of the error budget, pre-filtering of the MSS is useful for diagnostic purposes.

However, for standard spatial averaging filters, any advantage from spectral pre-filtering of the MSS decreases with increasing degree L and is therefore marginal for an MDT based on the GOCE gravity model. Hence, the first, most straightforward approach is the one taken here. In this case, the filtered MDT estimate is given by applying a filter F on the height residuals in Eq. (2):

$$\hat{\zeta} = F \circ (\zeta + \Delta N_L + \delta_L) \quad (3)$$

The best estimate in a least squares sense

$$\begin{aligned} \| \zeta - F \circ (\zeta + \Delta N_L + \delta_L) \| &= \| \zeta - F \circ \zeta - F \circ \\ &\quad (\Delta N_L + \delta_L) \| \\ &\leq \| \zeta - F \circ \zeta \| + \| F \circ \\ &\quad (\Delta N_L + \delta_L) \| \end{aligned} \quad (4)$$

is obtained when the filtering minimizes the attenuation and distortion of the MDT, while adequately suppressing the noise due geoid omission and commission errors. In the analysis below, we use a truncated Gaussian filter. For such a filter the degree of smoothing is proportional to the filter width, usually specified in terms of the filter's half-weight radius (HWR), which is the radius at which the Gaussian curve that defines the weighting function has fallen to half of its value at the origin. Choosing the correct filter radius is crucial for minimising the degree of attenuation of the MDT and is therefore discussed in some detail below.

Once the MDT has been calculated it can be used to determine the surface geostrophic currents, which are of ultimate interest to oceanographers. If accelerations and friction terms are neglected and horizontal pressure gradients in the atmosphere are absent, then the components of the surface geostrophic currents (u, v) are obtained from the MDT by

$$u = -\frac{\gamma}{fR}\frac{\partial \zeta}{\partial \phi}, \quad v = \frac{\gamma}{fR\cos\phi}\frac{\partial \zeta}{\partial \lambda} \quad (5)$$

where $f = 2\omega_e \sin\phi$ is the Coriolis force coefficient, ω_e is the angular velocity of the Earth, R is the mean radius of the Earth, ϕ is the latitude, λ is the longitude and γ is the normal gravity. Note that because the currents depend on the spatial derivatives of the MDT, noise in the MDT will be amplified in the estimated currents. Furthermore, because f approaches zero at the equator this noise will be further amplified at low latitudes. This emphasises the importance of ensuring noise is removed from the MDT before reasonable estimates of the circulation can be obtained.

2.1 The mean sea surface

To calculate the geodetic MDTs used in this study we use the DTU10MSS which is an update of the DNSC08MSS model (Andersen and Knudsen 2009). The DTU10MSS is the time-averaged ellipsoidal height of the ocean's surface computed from a combination of satellite altimetry using a total of 8 different satellite missions now covering a period extended to 17 years (1993–2009). The MSS has been derived using a 2-step procedure whereby a coarse long-wavelength MSS is initially determined from 17 years of temporally averaged mean profiles from TOPEX and JASON-1 merged with the adjusted 8-year mean profiles from ERS-2 and ENVISAT. The adjusted mean refers to the fact that the ERS-2 and ENVISAT data are initially fitted onto the 12-year mean of

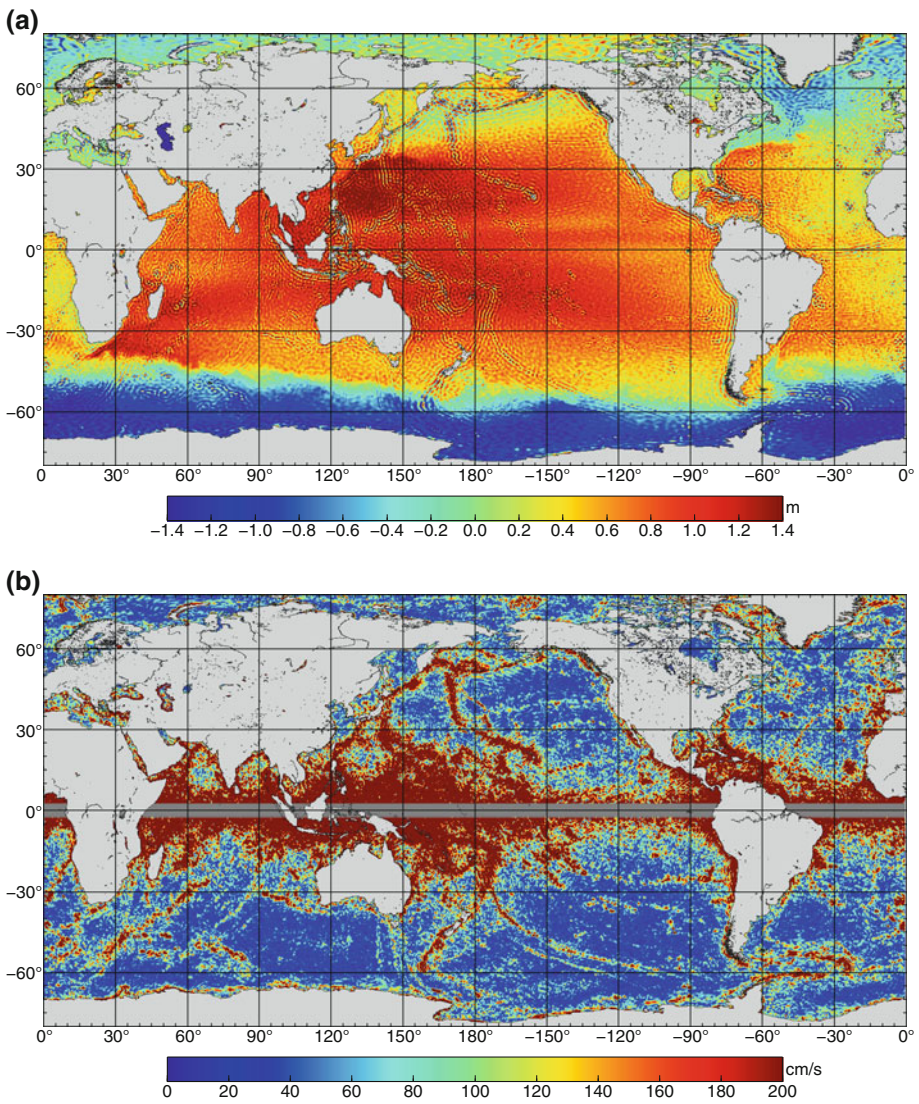

Fig. 1 **a** The unfiltered GOCE MDT, computed by subtracting the GOCE DIR geoid from the DTU10MSS. **b** Surface geostrophic current speeds calculated from the unfiltered GOCE MDT

TOPEX+JASON-1 to ensure that no systematic differences between the two datasets remain. Subsequently, retracked altimetry from the Geosat and ERS-1 Geodetic Mission is added using a remove–restore technique with respect to the coarse long wavelength MSS (Andersen et al. 2010). This procedure means wavelengths with spatial scales down to roughly 15 km are resolved in the final DTU10MSS product. Unlike other available products, the MSS is nearly global in coverage. In particular, the MSS of the Arctic Ocean to 86°N has been mapped by including laser altimetry from the ICESat mission. Remaining polar gaps and grid points corresponding to land are filled by interpolation based on a geoid model.

2.2 The geodetic mean dynamic topographies

To calculate the GOCE MDT, the GOCE DIR gravity model was used to define the geoid to the maximum d/o of 240 relative to the same T/P reference ellipsoid and mean-tide system as the DTU10MSS. This was then subtracted from the MSS to give the unfiltered MDT shown in Fig. 1a. Even without filtering, the GOCE MDT looks quite reasonable. All of the gross features of the general circulation are clear, and even smaller scale details such as the Agulhas retroflection off the Cape of Africa are obvious. However, for the reasons described above, an attempt to calculate the geostrophic currents from this unfiltered MDT is unsuccessful (Fig. 1b). The amplitude of the noise when translated into effective ocean current speeds far exceeds that of any true currents. Notice how this noise, being due primarily to geoid omission error, mirrors the prominent features of the sea floor topography. This is particularly evident in the Pacific. Notice also how the noise is amplified toward the equator due to the latitudinal dependence of the Coriolis parameter.

To assess the performance of GOCE relative to that of GRACE, the EIGEN-GL04S1 gravity model is used to

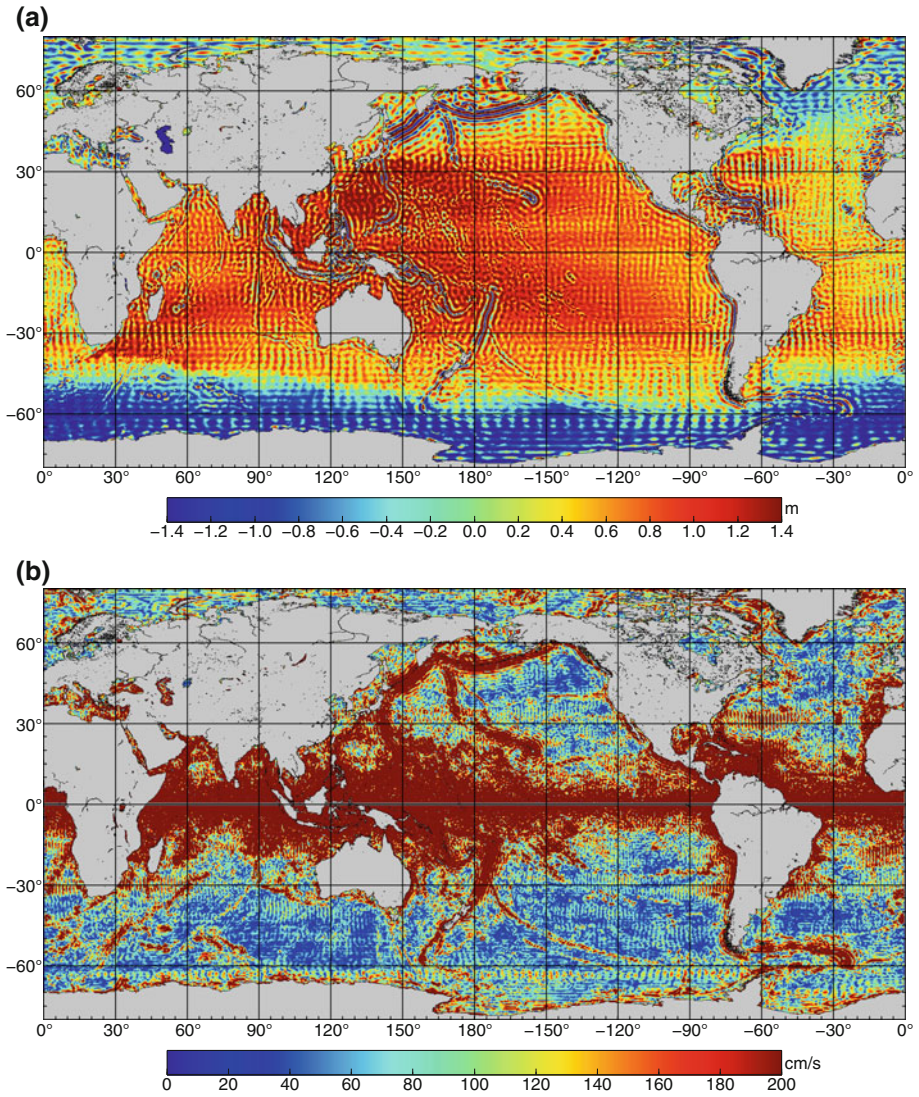

Fig. 2 **a** The unfiltered GRACE MDT, computed by subtracting the EIGEN-GL04S1 geoid from the DTU10MSS. **b** Surface geostrophic current speeds calculated from the unfiltered GRACE MDT

calculate a geoid to the maximum d/o of 150 relative to the same T/P reference ellipsoid and mean-tide system as the DTU10MSS. This was then subtracted from the MSS to give the unfiltered MDT shown in Fig. 2a. Again, the gross features of the ocean's circulation are obvious. However, both the geoid omission and commission errors are much larger for the GRACE MDT. As a result, the smaller scale features of the circulation are not as readily discerned. Unsurprisingly, the noise in the current field (Fig. 2b) is even greater than it is for GOCE.

Clearly to make a meaningful assessment of the geodetic MDTs and associated currents, both must be filtered. However, as mentioned previously, because spatial filtering, in addition to removing noise, also attenuates MDT gradients associated with ocean currents to a degree that is proportional to the filter width, it is important to find the minimum filter radius that will adequately remove the noise, thus preserving, as far as possible, the oceanographic content of the MDT. One approach to finding this minimum sufficient radius is to repeatedly filter the MDT while gradually increasing the filter radius to find the radius at which, by visual inspection, the seemingly unrealistic short scales have been removed from the MDT. However, there is clearly an element of subjectivity in this process, which is undesirable when trying to demonstrate the superiority of one geodetic MDT over another, as we are attempting here. Unless an objective measure can be found, one is always open to the accusation of selecting the filter radii to exaggerate the difference between two MDTs, thereby making an improvement seem greater than it, in reality, is.

With objectivity in mind, the approach to finding the optimum filter radius for each of the geodetic MDTs adopted here is to take the Maximenko MDT as our ground truth. In fact, rather than compare MDTs we compare current speeds.

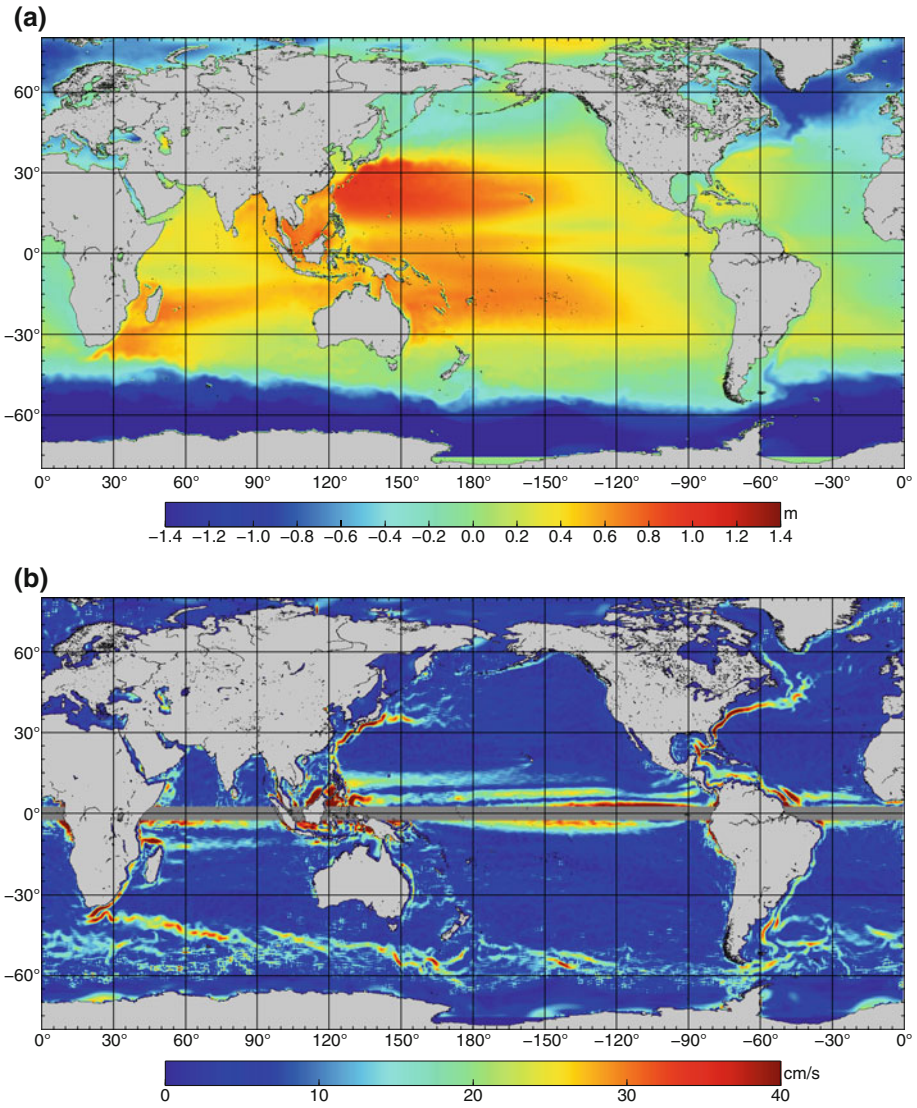

Fig. 3 **a** The Maximenko MDT, and **b** the surface geostrophic current speeds calculated from the Maximenko MDT

This focuses the analysis on the short spatial scales where noise in the geodetic MDT is a problem and where the Maximenko MDT is likely to be more accurate. This is a reasonable assumption as we can be confident, at least at this stage of the GOCE mission, that the currents obtained from the Maximenko MDT, which incorporates in-situ drifter data, are more reliable than those from GOCE. As Fig. 3 shows, the Maximenko MDT is free from small-scale noise afflicting the geodetic MDTs and the ocean currents are clearly defined. To find the optimum filter radius for a particular geodetic MDT we calculate for some region the RMS difference between the Maximenko currents with those calculated from the geodetic MDT over a range of filter radii and select the filter width that minimises the difference between the two. With no filtering, the difference will be dominated by the noise in the geodetic MDT. As the filter width is increased, the difference due to this noise will gradually be reduced. However, the difference due to the attenuation of the geodetic MDT by the filter will gradually grow. At some point, the two contributions will cross each other. This cross-over point defines the ideal filter width.

Following this approach, we find that the RMS difference between the GOCE and Maximenko current speeds computed over the North Pacific initially falls rapidly with increasing half weight radius of the Gaussian filter (Fig. 4). A minimum RMS residual of about 6 cm/s is reached for a filter half-width radius of 140 km. Beyond this the difference between the currents derived from the filtered GOCE MDT and the Maximenko currents begins to increase again, reflecting the fact that beyond this filter width, the attenuation of the MDT and currents by the filtering begins to outweigh the benefit of reduced noise. Hence, for the evaluations that follow, the GOCE MDT was filtered with a 140- km isotropic truncated Gaussian filter.

In Fig. 4 we also plot the RMS residual for the GRACE MDT. Again, the RMS difference decreases rapidly with

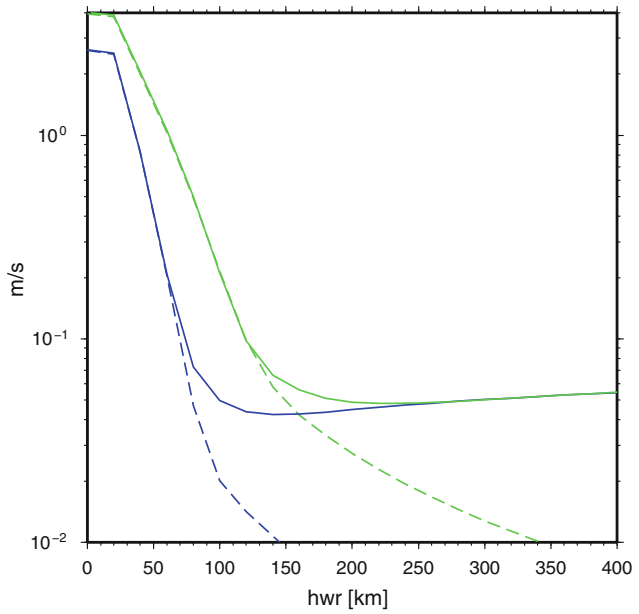

Fig. 4 The RMS difference (calculated for the North Pacific region 140–220E, 10–50N) between an estimate of the current speeds which includes in-situ data and the GOCE (*blue*) and GRACE (*green*) estimate of these currents as a function of filter half-weight radius. A model of the omission error implied current speeds as a function of filter radius for geoid truncations at 240 (*blue dashed*) and 150 (*green dashed*)

increasing filter width. However, the initial unfiltered difference is almost twice that for the GOCE MDT, reflecting the fact that the unfiltered GRACE MDT is much noisier than the unfiltered GOCE MDT. The RMS decline with increasing filter width is somewhat less steep than is the case for the GOCE MDT, and a minimum RMS residual of about 7 cm/s occurs with a filter radius of about 200 km. Hence, for the evaluations that follow, the GRACE MDT was smoothed with a Gaussian filter of this half-weight radius. It is worth emphasising that the superiority of GOCE over GRACE, at least in terms of ocean currents, rests on this difference in the required filter width (140 vs. 200 km).

For both geodetic MDTs, the dominant error source is geoid omission error. To illustrate this we model the impact of the geoid omission error on the estimated currents by passing the MSS through a spectral filter (this is done by expressing the MSS as a series of spherical harmonic coefficients and then reconstituting the MSS geographically from the series, with truncation at some degree and order). The residual, upon subtracting the spectrally filtered MSS from the original MSS, is then filtered in the same way as the geodetic MDTs, and pseudo ocean currents are calculated from this residual according to Eq. 5. In Fig. 4 the RMS of the implied geostrophic current speeds is plotted as a function of filter width for the case where the spectrally filtered MSS was truncated at d/o 240 (blue dashed) and at d/o 150 (green dashed). The close correspondence between the dashed curves and the curves from the filtered geodetic MDTs computed with geoids truncated at the same values shows that the dominant error source for both MDTs is indeed geoid omission error.

3 Evaluation

In this section we evaluate the geodetic MDTs, filtered as described above, and the associated geostrophic currents, against the combined Maximenko MDT. We start with a global overview of the MDTs and associated currents, before considering several regions of special interest in more detail.

The GOCE MDT filtered with a 140-km Gaussian filter, together with the associated geostrophic currents, is shown in Fig. 5. Clearly, the filter has effectively removed the noise in the unfiltered MDT (Fig. 1). However, the true impact of the filtering is revealed in the map of ocean currents. Features of the sea floor topography have been removed, and all of the major ocean currents are now clear. Maximum current speeds are of the order of 40 cm/s (note the reduction of scale compared with Fig. 1b). The current field looks reasonable, albeit a little weaker, when compared with the MAX09 currents (Fig. 3b). It is particularly interesting to note the good agreement with regard to the equatorial currents of the Pacific, given the degree to which this region was contaminated by noise in the unfiltered MDT. There is little to distinguish the GOCE MDT from the GRACE MDT filtered with the 200-km filter (Fig. 6a). However, the estimated currents (Fig. 6b), while free from the noise that afflicted the currents estimated from the unfiltered MDT, are noticeably weaker than those from the GOCE or Maximenko MDTs, with peak speeds outside of the equatorial latitudes of around 25 cm/s, compared with around 40 cm/s for the GOCE currents. Apparent currents around islands, particularly those of the Indonesian flow through region, and around Hawaii, are not realistic, but result from issues in defining the land/sea boundary.

These visual impressions are confirmed in the top band of statistics in Table 1. Once the global mean offset between the MAX09 and geodetic MDTs (clear from a comparison of Figs. 3 and 5 or 6) has been removed, the RMS difference between the geodetic MDTs and MAX09 is around 6 cm, with the GOCE MDT marginally closer. In terms of current velocities the GOCE MDT is in better agreement with MAX09. Interestingly, for both of the geodetic MDTs there is a marked difference between the u and v velocity components, with the agreement much better for the former than for the latter. The reason for this is that while the global RMS differences relative to MAX09 are similar for both the zonal and meridionally currents, the meridional currents have a smaller RMS than the zonally currents (9 vs. 13 cm/s for MAX09), and so errors due to noise will have a greater impact on the total skill for the meridional currents.

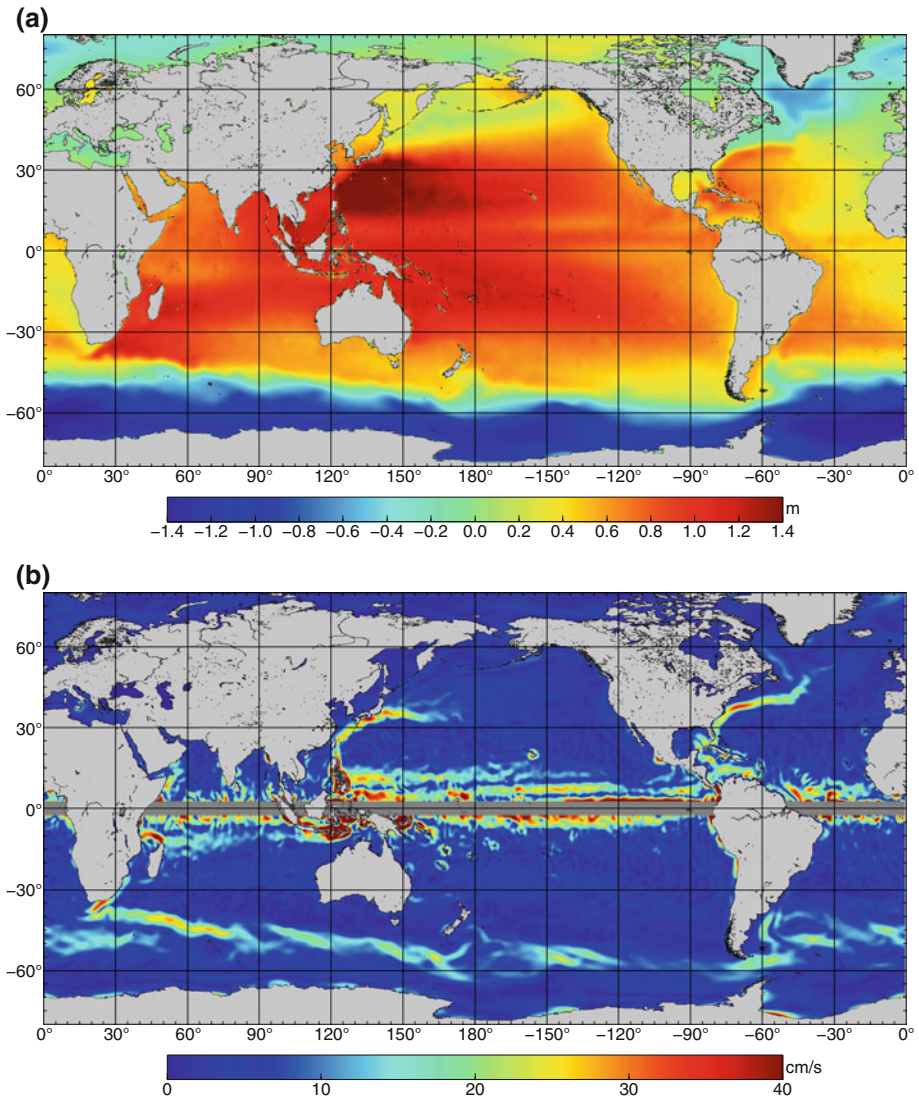

Fig. 5 **a** The GOCE MDT filtered with a 140-km Gaussian filter. **b** Surface geostrophic current speeds calculated from the filtered GOCE MDT

Table 1 also provides summary statistics for each of the regions that will be discussed in more detail below. Each region generally mirrors the pattern seen globally. In terms of the MDTs themselves, there is little to distinguish the geodetic estimates, either from themselves of from MAX09, as reflected in the fact that all skill and correlation scores for height exceed 0.98. In terms of the RMS differences, in each case the GOCE MDT is fractionally closer to MAX09, reflecting the greater attenuation of the GRACE MDT due to the more severe filtering required to smooth it. The offsets, which reflect the longest wavelength differences between the MDTs, are at the centimetre level. The ranking of the magnitudes of the offsets are consistent between the GOCE and GRACE MDTs, ranging from about 3 cm for the North Atlantic to 1 mm for the Southern Ocean. Since the geodetic MDTs are produced by the same MSS, which is different to the MSS used in the geodetic part of MAX09, this is most likely due to long-wavelength MSS differences.

Mirroring the global statistics, for all regions, the RMS difference between the GOCE and MAX09 MDTs is less than the difference between the GRACE and MAX09 MDTs. And this is true of both the u and v velocity components. For the u component the per cent of spatial variance in MAX09 accounted for by the GOCE MDT (i.e. skill) ranges from a minimum of 70% for the North Atlantic to a maximum of 76% for the North Pacific. In all cases, the GRACE u-velocity component accounts for less of the variance in the MAX09 u component. The greatest difference is seen in the North Atlantic, where the GRACE MDT accounts for 17% less variance, while the smallest difference is seen in the Southern Ocean where GRACE accounts for 70% of the variance in the MAX09 u component compared with 72% for GOCE. Similarly, for the v component GOCE accounts for more of the spatial variance in MAX09 for all regions, although, just as for the global case, the skill scores for the v component are lower than for the u component. They range from maximums

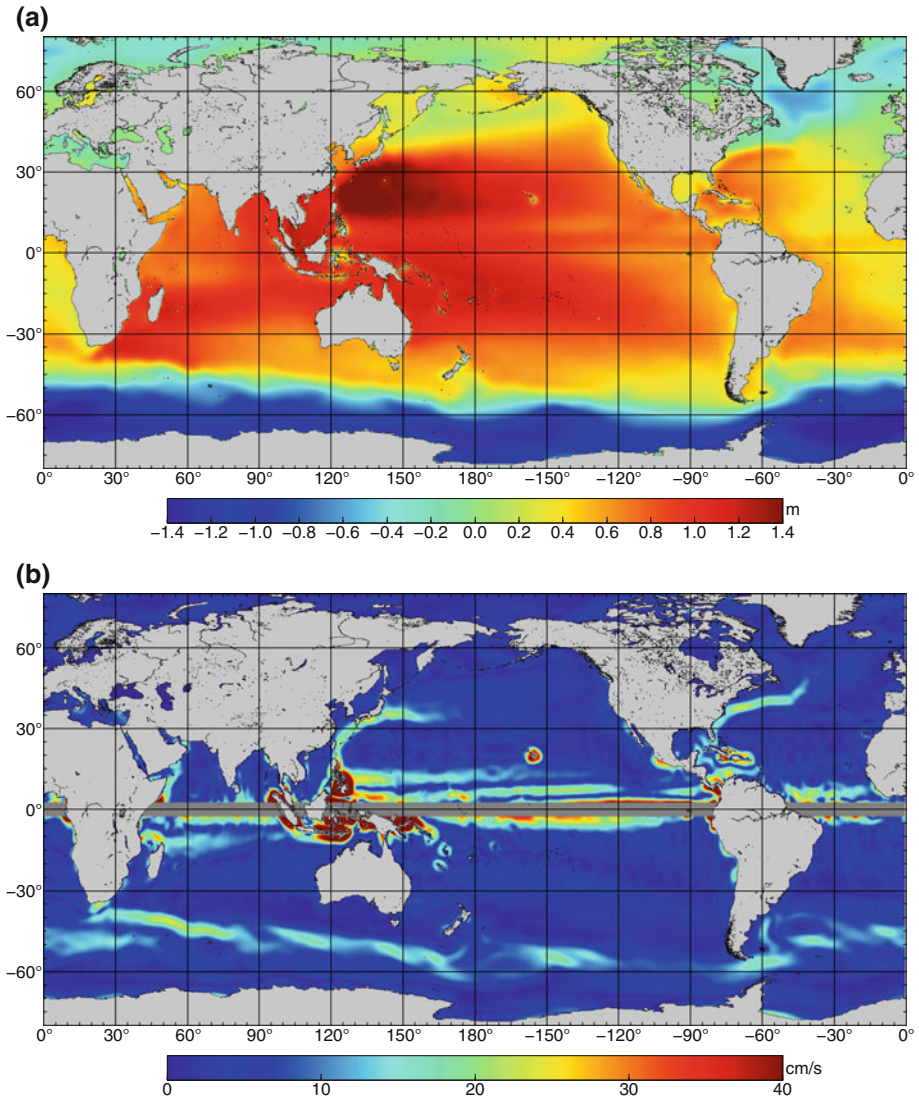

Fig. 6 **a** The GRACE MDT filtered with a 200-km Gaussian filter. **b** Surface geostrophic current speeds calculated from the filtered GRACE MDT

of 49 and 36% for GOCE and GRACE in the North Atlantic, to minimums of 30 and 24% for GOCE and GRACE in the Southern Ocean. The greatest difference between the GOCE and GRACE is found in the Agulhas region where GOCE has a skill of 45% compared with 26% for GRACE.

In summary, these statistics show that GOCE more closely matches the combined solution for all regions and for both components of the velocity vector. However, there are some interesting regional variations in the degree to which GOCE out performs GRACE, as well as differences between the u and v components. The reasons for these differences are a reflection of the predominant orientation of the currents for a particular region: for all regions the u component dominates, but, for instance, the currents are more meridionally oriented in the North Atlantic, meaning this region has the best skill scores for the v components, while the Southern Ocean is most strongly zonal, and therefore it has the worst skill scores for the v component. However, further study is required to fully understand these regional variations in statistics.

3.1 The North Atlantic region

The Gulf Stream is one of the most important and strongest of the world's currents. By feeding large volumes of relatively warm water from the tropics into the North Atlantic Current, where it is transported to higher latitudes, it plays a critical role in regulating the Earth's climate (Manabe and Stouffer 1999). The Gulf Stream begins upstream of Cape Hatteras near 30°N and ends east of the Grand Banks at about 40°N, 50°W. Along this path, due to recirculations and entrainment, the transport of the Gulf Stream increases quite rapidly from about 30 Sv at its initiation to 150 Sv at Grand Banks (Hogg and Johns 1995). The width of the Gulf Stream

Table 1 Statistics summarising the differences between the GOCE (top row of each italic emphases region) and the GRACE (bottom row of each italic emphases region) MDTs and the Maximenko MDT

	Offset	Height (cm)			*U* velocity (cm/s)			*V* velocity (cm/s)		
		RMS	Skill	Cor	RMS	Skill	Cor	RMS	Skill	Cor
Glbl	∗	*6.10*	*0.99*	*1.00*	*9.04*	*0.55*	*0.77*	*8.97*	*0.06*	*0.43*
	∗	*6.31*	*0.99*	*1.00*	*10.02*	*0.44*	*0.71*	*9.62*	*−0.08*	*0.35*
NA	−2.82	4.91	0.98	0.99	1.65	0.70	0.84	1.88	0.49	0.70
	−2.86	5.60	0.98	0.99	2.07	0.53	0.73	2.11	0.36	0.60
NP	*−0.41*	*4.96*	*0.99*	*1.00*	*1.56*	*0.76*	*0.88*	*1.69*	*0.42*	*0.65*
	−0.24	*5.18*	*0.99*	*0.99*	*1.74*	*0.71*	*0.84*	*1.84*	*0.31*	*0.56*
AG	1.74	5.11	0.99	0.99	2.23	0.73	0.86	2.16	0.45	0.67
	1.90	5.79	0.98	0.99	2.66	0.62	0.79	2.50	0.26	0.51
BM	*0.65*	*7.15*	*0.99*	*0.99*	*1.54*	*0.71*	*0.84*	*2.10*	*0.36*	*0.61*
	0.78	*7.32*	*0.99*	*0.99*	*1.79*	*0.63*	*0.79*	*2.29*	*0.24*	*0.50*
SO	−0.11	8.12	0.99	0.99	4.10	0.72	0.85	4.36	0.30	0.55
	0.06	7.73	0.99	0.99	4.26	0.70	0.84	4.56	0.24	0.49

Statistics are given for the global ocean excluding the equator (Glbl), the North Atlantic (NA), the North Pacific (NP), the Agulhas region (AG), the Brazil-Malvinas Confluence region (BM) and the Southern Ocean (SO). The extent of the regional domains are as in the corresponding regional maps (Figs. 6, 7, 8, 9, 10 and 11). For the MDT height the RMS is computed after removal of the regional offsets. For all quantities, skill is the per cent of the spatial variance accounted for, and cor is the spatial correlation

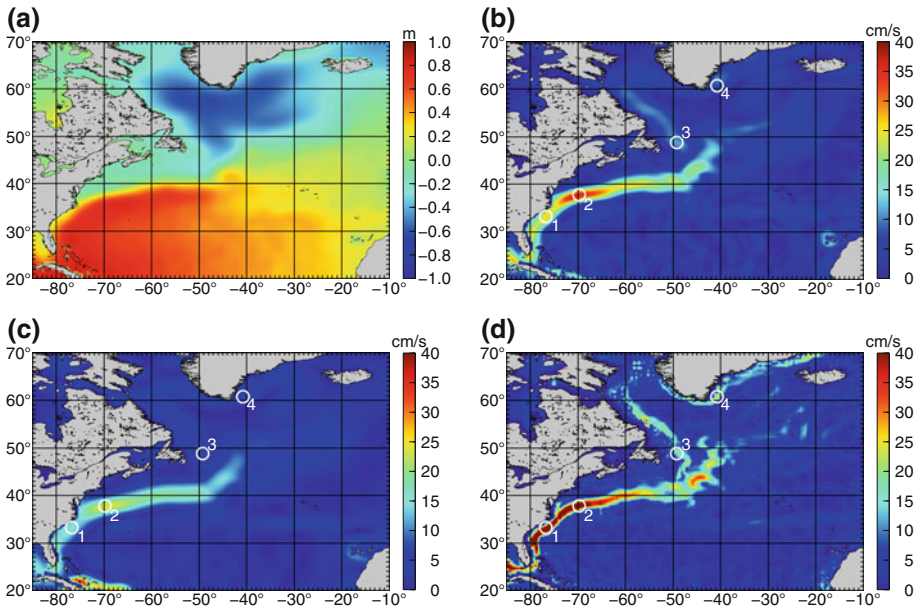

Fig. 7 **a** The North Atlantic GOCE MDT. Geostrophic current speeds from **b** GOCE, **c** GRACE, and **d** Maximenko

is in places no more than 90 km, but core peak velocities can be greater than 2 m/s.

The MDT of the Gulf Stream region (Fig. 7) is characterised by heights up to about 70–90 cm in the middle of the subtropical gyre, rapidly decreasing to zero north of the current. This sharp front is a reflection of the strength of the Gulf Stream. We can roughly consider the Gulf Stream as consisting of two parts. For the first part, between 30°N and 36°N the Gulf Stream exists as a narrow western boundary current, following closely the US east coast. Here, the GOCE-derived mean current speed reaches a maximum of 26 cm/s off Cape Hatteras (location NA1; all locations referred to are marked on the appropriate regional current map, and the coordinates and current speeds are given in Table 2). This is somewhat less than the 45 cm/s derived from MAX09, but much more reasonable than the 15 cm/s obtained from GRACE. It is

Table 2 MDT heights and current speeds at twenty locations (four for each the five regions) for the Maximenko (Max), GOCE and GRACE MDTs

	Location		Height (cm)			Current speed (cm/s)		
	Lat	Lon	Max	GOCE	GRACE	Max	GOCE	GRACE
NA1	*33*	*−77*	*−23*	*12*	*18*	*45*	*26*	*15*
NA2	*38*	*−70*	*−10*	*−8*	*−5*	*47*	*36*	*24*
NA3	*49*	*−49*	*−74*	*−70*	*−70*	*14*	*11*	*7*
NA4	*61*	*−41*	*−97*	*−81*	*−80*	*25*	*8*	*5*
NP1	27	126	55	80	81	37	27	19
NP2	33	136	72	84	84	45	37	23
NP3	35	147	53	67	70	30	27	21
NP4	44	155	−24	−14	−12	13	7	4
AG1	*−27*	*34*	*31*	*52*	*56*	*32*	*18*	*13*
AG2	*−36*	*24*	*44*	*56*	*50*	*57*	*27*	*16*
AG3	*−40*	*22*	*12*	*45*	*38*	*45*	*26*	*15*
AG4	*−39*	*37*	*25*	*43*	*42*	*29*	*22*	*19*
BM1	−30	−47	14	36	38	20	6	2
BM2	−43	−59	−36	−19	−15	32	22	14
BM3	−40	−53	−19	3	2	33	15	10
BM4	−48	−39	−72	−54	−57	33	24	18
SO1	*−45*	*69*	*−50*	*−23*	*−23*	*29*	*28*	*22*
SO2	*−55*	*164*	*−72*	*−45*	*−45*	*42*	*25*	*18*
SO3	*−56*	*−144*	*−106*	*−87*	*−86*	*40*	*24*	*19*
SO4	*−56*	*−56*	*−90*	*−70*	*−72*	*28*	*23*	*18*

For each region locations are marked on the corresponding regional maps (Figs. 6, 7, 8, 9, 10 and 11)

worth pointing out, however, that while MAX09 gives quite consistent current speeds along this boundary section, GOCE does not. This will require further investigation.

At about 36°N, for reasons that are still not fully understood dynamically, the Gulf Stream separates from the boundary and starts to flow due east. The estimated current speeds from GOCE at 70°W (location NA2) are approximately 36 cm/s compared with only 24 cm/s from GRACE. This compares with 47 cm/s from MAX09. Therefore, we see again that GOCE comes closer to the estimate that uses in-situ observation. To the east of about 60°W, the Gulf Stream becomes broader and less intense. This transition is much clearer in GOCE than in GRACE. At about 38°N, 44°W the Gulf Stream encounters the Mann Eddy (Mann 1967), a permanent recirculation where the Gulf Stream bifurcates into the eastward flowing Azores current (Gould 1985), and the northerly flowing North Atlantic Current. This eddy is clearly visible as the positive bump in the GOCE MDT. The circulation around the Mann Eddy is most intense on its Northern flank. In this respect, the GOCE currents come much closer to the MAX09 estimate, showing the ability of GOCE to better resolve the finer scale features of the ocean's circulation.

The boundary currents of the sub-polar gyre, although weaker than the Gulf Stream, are nonetheless an important component of the North Atlantic circulation. Due east of Newfoundland (location NA3) MAX09 gives a Labrador Current speed of 14 cm/s. The GOCE estimate is similar at 11 cm/s, while the GRACE estimate is only 7 cm/s. Near the southerly tip of the East Greenland Current (location NA4), the current speeds from the geodetic MDTs are both less than 30% of the speed given by MAX09, with the GOCE estimate marginally greater than the GRACE estimate. This is most likely because this current is particularly narrow and therefore more attenuated by the filtering.

3.2 The Kuroshio region

The Kuroshio current is the strong western boundary current of the North Pacific subtropical gyre, in some respects analogous to the Gulf Stream in the North Atlantic. It flows northeast from Taiwan and along the eastern coast of Japan following the continental slope. Peak current speeds within the Kuroshio can reach 1 m/s and it has a width of about 150 km. At about 36°N the Kuroshio Current leaves the boundary and begins to flow east into the North Pacific as the Kuroshio Extension. This current is a free jet and forms the boundary between the subtropical and subpolar gyres. Although not as directly connected to the global overturning circulation as the Gulf Stream, the Kuroshio, through

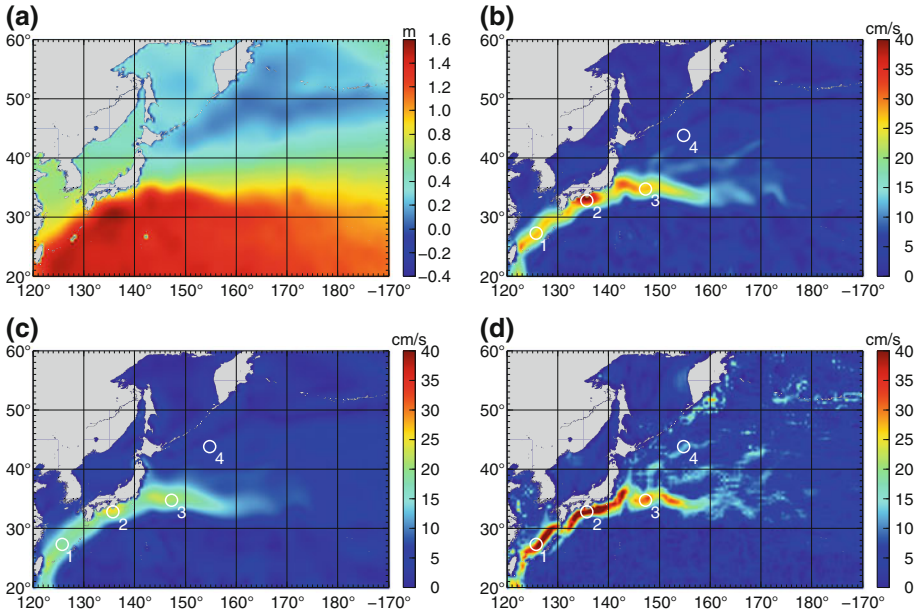

Fig. 8 **a** The North Pacific GOCE MDT. Geostrophic current speeds from **b** GOCE, **c** GRACE, and **d** Maximenko

vigorous heat exchange with the atmosphere, plays an important role in governing the climate variability of the region and North America, through for instance the Pacific Decadal Oscillation.

For the Kuroshio region (Fig. 8) the MDT decreases from a high of about 140 cm in the middle of the subtropical gyre to a low of about −20 cm in the sub-polar gyre. The Kuroshio Extension is known to exhibit quasi-stationary meanders as it flows east. These are visible as kinks in the sharp MDT gradient just east of Japan. According to MAX09, the mean current speed in the Kuroshio Current between Taiwan and Japan is 37 cm/s (location NP1). GOCE does not give as clear a picture of the boundary current here: current speeds are somewhat weaker (27 cm/s) and not as consistent or as well defined. This is similar to what was found for the Gulf Stream boundary current and suggests that for such narrow boundary currents care must be taken if their details are to be accurately recovered from GOCE. Nevertheless, it is clear from Fig. 8 that GOCE still provides an estimate of the speed and width of the current that is closer to the "truth" than what is obtained from GRACE (19 cm/s). Along the outer coast of Japan (location NP2), the Kuroshio Current is somewhat broader and stronger, and we find quite close agreement between the GOCE and Maximenko current speeds, with each close to 40 cm/s. In contrast, the current speed from GRACE is closer to 20 cm/s. An interesting small detail, which shows the improvement in resolution provided by GOCE, is the kink in the Kuroshio Current where is deflected east by the southern tip of Japan. This is resolved by GOCE but not by GRACE.

At 36°N, the Kuroshio Current meets the Oyashio Current —the southerly flowing boundary current of the North Pacific subpolar gyre—where upon it leaves the boundary to flow east into the North Pacific as a free jet. As pointed out above for the MDT, the Kuroshio Extension meanders vigorously to the north and south. These excursions are associated with local accelerations of the current. This is clear in both the GOCE and Maximenko current fields, which are in relatively close agreement in terms of form and magnitude. Again, these features cannot be seen in the currents from GRACE. To the north and to the east of the Kuroshio extension the flow breaks down into finer scale structures. Comparing the GOCE and Maximenko current fields we find many similarities in the form and amplitude of these features—detail that is almost completely absent from the GRACE current field. Comparison of current speeds at locations NP3 and NP4, as given in Table 2, confirms this visual impression.

3.3 The Agulhas region

The Agulhas Current flowing around the southern horn of Africa, by providing a route for warm water out of the Indian Ocean and into the Atlantic, is an important link in the global overturning circulation. Recent studies suggest that the variability of this current system may exert a controlling influence of the Atlantic meridional overturning circulation (MOC) and through this impact on climate (Friocourt et al. 2005; Biastoch et al. 2009). The western boundary current of the South Indian gyre forms the first part of the southward flowing Agulhas Current. At the southern tip of Africa, the Agulhas Current flows west toward the Atlantic, before interaction with the ACC forces the Agulhas to turn back on itself, in what is known as the Agulhas retroflection; a unique feature of the ocean's circulation. At regular intervals, eddies, known as Agulhas rings, are pinched off from the retroflection. In doing so, warm water from the Indian Ocean is fed

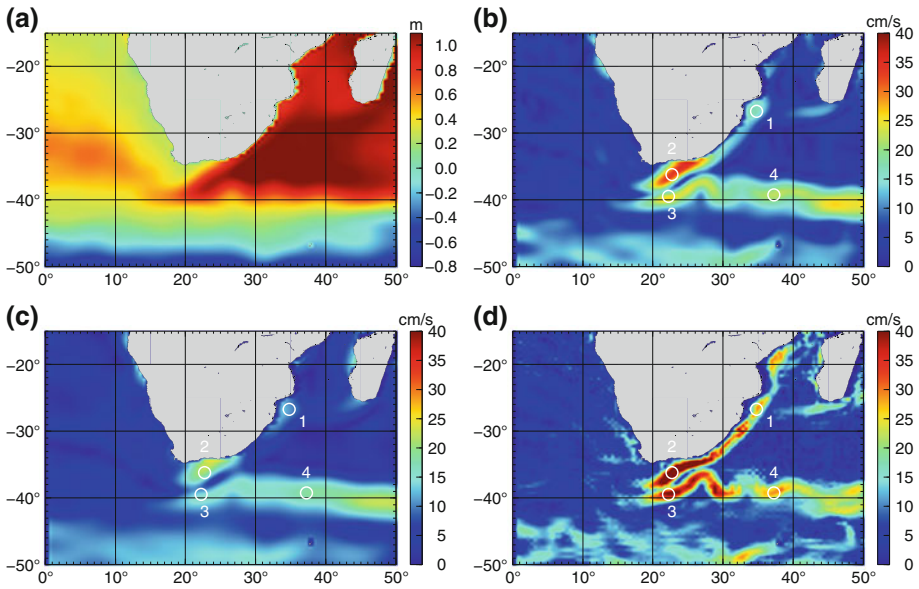

Fig. 9 **a** The GOCE MDT for the Agulhas region. Geostrophic current speeds from **b** GOCE, **c** GRACE, and **d** Maximenko

into the Atlantic. The easterly flowing return branch of the Agulhas current is known as the Agulhas Return Current. Like the Gulf Stream, in-situ observations show that peak current speeds within the core of the Agulhas Current can reach 2 m/s (Boebel et al. 1998) and the transport of the Agulhas Current has been estimated to be between 70 and 80 Sv (Donohue et al. 2000; Bryden et al. 2005).

The MDT of the Agulhas region (Fig. 9) is characterised by values up to about 1 m in the middle of the South Indian gyre decreasing to −1.5 m south of the ACC. The Agulhas Current flowing south along the African continental slope is clearly visible as a continuous boundary current in the GOCE current field but less so in the currents derived from GRACE. At location AG1 the current speed obtained for MAX09 is 32 cm/s, compared with 18 cm/s from GOCE and 13 cm/s from GRACE. As the Agulhas Current rounds the tip of Africa, interaction with the ACC causes the current to turn back on itself. This retroflection is visible in the GOCE MDT as the finger of high values protruding into the South Atlantic. Here the mean current speeds of the Agulhas Current are at their greatest. For the MAX09 estimate, maximum current speeds are 57 cm/s for the westward-flowing component of the Agulhas (location AG2) and around 45 cm/s for the more southern return flow (location AG3). The current speeds from GOCE are about 20 cm/s less for each location, whereas for GRACE they are about 30 cm/s less. Also the location of the current cores are much more well defined for GOCE compared with GRACE and more closely resemble those from MAX09.

The Agulhas Return Current is manifested in the MDT as the sharp boundary between high (red) and low (green) values that runs almost zonally to the southeast of the African horn. Here we find that GOCE captures the quasi-stationary meanders of this current, visible as the kinks in the MDT. These meanders, which are associated with enhanced current speeds, are clear in both the GOCE and Maximenko current fields but not so well defined in the currents obtained from GRACE (e.g. location AG4). The strong currents in the lower right of Fig. 9 are part of the ACC and will be described below.

3.4 The Brazil-Malvinas Confluence region

The Brazil-Malvinas Confluence region is located in the south-western Atlantic where the northward flowing Malvinas Current collides with the southward flowing Brazil Current. It is one of the most energetic regions of the world's oceans (Chelton et al. 1990; Fu et al. 2001), and, as such, the circulation of this region is rich in detail, thus providing a strong test of the geodetic MDT calculation. The MDT in the Brazil-Malvinas Confluence region (Fig. 10) is characterised by values up to about 60–80 cm in the subtropical gyre decreasing to −1.5 m on the southern side of the ACC. The Malvinas Current is a northward-flowing offshoot of the ACC with a width of about 100 km. It follows the Argentine shelf edge between 50°S and 36°S. This path is reflected in the positive MDT values on the shelf. The path of the Malvinas Current, travelling initially west to the north of the Falkland Islands, before turning to flow northeast along the shelf edge is clear in the currents from GOCE, but much less so in the currents from GRACE. The peak current speed along the path of the Malvinas Current (location BM2) from GOCE is 22 cm/s, compared with 32 cm/s from MAX09. The core of the current is also somewhat more blurred in the GOCE estimate. As for the other regions considered, this is not surprising given that the latter contains in-situ observations and has not been filtered. In comparison with GRACE,

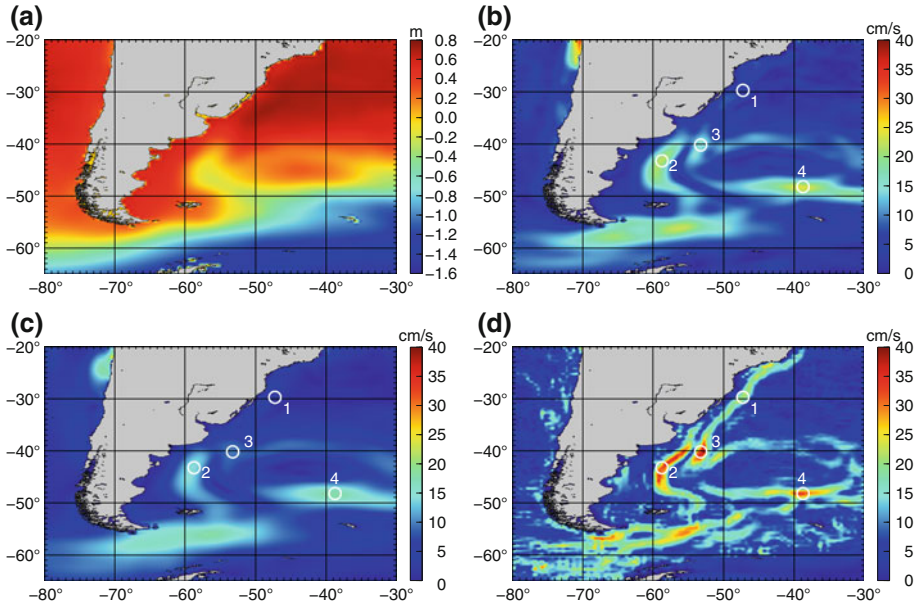

Fig. 10 **a** The GOCE MDT for the Brazil-Malvinas Confluence regions. Geostrophic current speeds from **b** GOCE, **c** GRACE, and **d** Maximenko

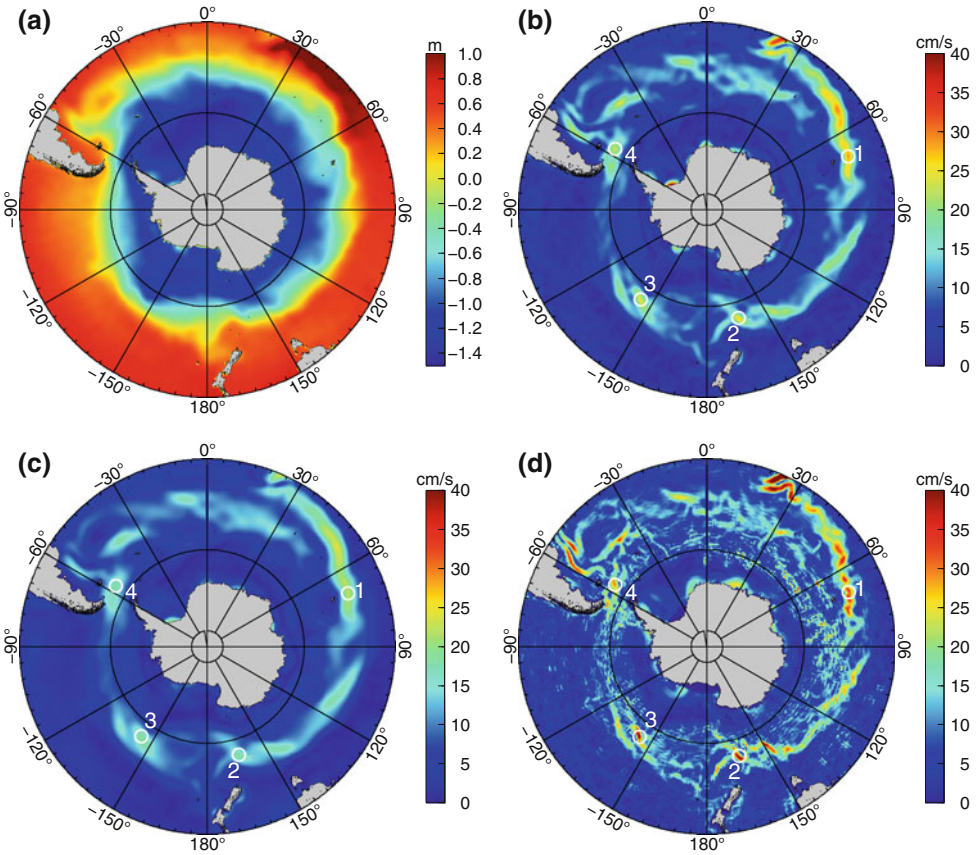

Fig. 11 **a** The Southern Ocean GOCE MDT. Geostrophic current speeds from **b** GOCE, **c** GRACE, and **d** Maximenko

we again find that GOCE gives a clearer and more realistic picture of this current.

The region of high MDT values against the Argentine shelf converges to a point at 36°S. This corresponds to the point where the Malvinas current collides with the Brazil Current. Although the southward-flowing Brazil Current (location BM1) is clearly present in the MAX09 current map (20 cm/s), it is faint even in the GOCE current field (6 cm/s). After the collision between the Malvinas and Brazil Currents part of the Brazil Current recirculates, while part continues south in

what is known as the Brazil Current overshoot, before turning back at 45°S, 55°W to flow equator-ward in a north-easterly direction (Saraceno et al. 2004). This overshoot is manifested as the 'V' shape at the specified location. This feature of the Brazil Current can be discerned in the GOCE current field and compares reasonably well in terms of structure with the estimate from MAX09 (e.g. location BM3). In contrast, this feature is not clear in the GRACE based currents. The confluence also causes the Malvinas Current to loop back on itself and rejoin the ACC at its sub-Antarctic front. To the south of the Brazil Current overshoot it is just possible to make out this return flow in the MAX09 and GOCE currents. The maximum current speeds of this region are found in the ACC sub-Antarctic front at about 50°S, 40°W (location BM4). Here, there is relatively good agreement between the GOCE and Maximenko current fields in terms of both the location and magnitude, while for GRACE the currents are weaker.

3.5 The Southern Ocean region

Forced by strong zonal winds and unbounded by meridional continental boundaries, the Antarctic Circumpolar Current (ACC) is unique among the world's ocean currents. Although surface current speeds are only up to 20 cm/s, much less than many of the other currents described above, because the flow is close to barotropic, reaching depths of 4000 m, and up to 2000 km wide in places, it transports more volume than any other current. The estimated transport of the ACC is up to 150 Sv (Knauss 1996). By linking the three major ocean basins, the ACC is also an important pathway for the transportation of the heat and salinity and a crucial component in the overall regulation of the ocean's energy budget. Given the interaction between a strong barotropic flow and ocean floor topography, the ACC is also an important test bed for physical theories regarding the ocean's circulation, and, in particular, how topography torques balance the wind forcing to produce a steady flow.

It is in the Southern Ocean that we find the greatest height change in the MDT (Fig. 10). At the northern limit of our domain at 30°S the MDT has a typical value in excess of 1 m, while at the southern limit of the domain adjacent to the Antarctic coast the MDT has a typical value of around −1.5 m. The sense of this gradient corresponds to the eastwardly direction of the current. Just as for the other regions considered above, we find that overall the GOCE MDT comes much closer to the level of detail and current speeds obtained from MAX09, which includes in-situ observations. Excluding the Agulhas and the Malvinas-Brazil Confluence regions, the maximum mean current speeds of the ACC from the GOCE MDT are found in the Indian Ocean sector north of the Kerguelen Islands. Here there is good agreement between the GOCE and Maximenko current estimates both in terms of magnitude—about 30 cm/s for each—and spatial form (location SO1). According to MAX09, however, the maximum current speeds of 40 cm/s are seen further downstream south of New Zealand (location SO2) and near 150W (location SO3). Here the current speeds from GOCE are around 25 and 18 cm/s from GRACE. As for the other regions, in general, a greater level of detail can be resolved in the GOCE current field in comparison with that obtained from GRACE, and the magnitudes are closer to those of MAX09.

4 Concluding discussion

A key scientific goal of the GOCE mission is to deliver a model of Earth's gravity that will enable the ocean's time mean circulation to be determined globally with unprecedented spatial resolution. It is with the goal in mind that here we have presented an assessment of a mean dynamic topography and associated geostrophic surface currents derived from a preliminary GOCE gravity model. Our assessment of GOCE's performance is based on the GOCE DIR gravity model, and for comparison an MDT derived from the GRACE EIGEN-GL04S1 model, and an MDT from Maximenko et al. (2009) that combines a GRACE-based geodetic MDT estimate with in-situ drifter data to improve the short scales.

There is little to distinguish the MDTs themselves; all look similar with regard to the main features of the ocean's general circulation. This is not surprising since MAX09 is based on a GRACE model, and a GRACE model is used to constrain the longest wavelength of the DIR solution. Discounting any meaningless global offset, we find some basin-scale differences between the geodetic and Maximenko MDTs, with a maximum offset of about 3 cm over the North Atlantic. This most likely indicates long-wavelength differences in the MSS's used in the MDT calculations, rather than any gravity model differences. The centred pattern RMS differences between the GOCE MDT and MAX09, both global and regional, are generally a little less than is the case for the GRACE MDT, reflecting attenuation of the MDT by the greater degree of filtering required to smooth it, although the differences are small. An exception to this general pattern is the Southern Ocean where the GRACE MDT is closer to the Maximenko MDT. This is most likely due to a paucity of in-situ data in the Southern Ocean, meaning the Maximenko MDT deviates less from the GRACE MDT in this region than elsewhere.

Substantial differences between the MDTs are revealed by computing geostrophic currents from them. Being proportional to the gradient of the MDT, this emphasizes the short scales where the important differences between the MDTs lie. Overall, we find that the circulation estimated from the GOCE MDT is superior to that obtained from the GRACE-based MDT. Finer details of the ocean's circulation

are better resolved in the GOCE MDT and the current speeds, being greater, are closer to those obtained from MAX09. By the three statistical measures given in Table 1, both the u and v components of the GOCE velocity field are closer than those from GRACE to the MAX09 estimates. The strongest measure of similarity is skill—the per cent of spatial variance in the MAX09 currents accounted for by the geodetic currents. Globally, the GOCE currents account for just over 10% more of the spatial variance in the currents from the combined MDT compared with the GRACE currents. The ability of the geodetic MDTs to account for the spatial variance of the v component of the MAX09 currents is much poorer than for the u component, and this is shown in the spatial correlations as well. The fact the RMS differences are about the same for both components, however, shows that the noise is no worse for the v-component. Rather, the low skill scores reflect the fact that the ocean currents are primarily zonal in nature, and so any noise has a greater impact on the skill score. This especially becomes an issue towards the equator, leading to the almost zero global skill scores for the v component of the velocity field. This suggests that it would be appropriate to increase the zonal width of the filter toward the equator.

Having looked closely at several important current systems, a consistent picture emerges: The currents derived from the GOCE MDT are generally stronger and more clearly defined than those derived from the GRACE MDT. Looking at actual current speeds for the 20 locations given in Table 2 (four locations for each of the five regions), in all cases the current speeds estimated from GOCE are greater than those from GRACE. In absolute terms, the improvements range from 3 cm/s at locations NA4 (the East Greenland Current) and AG4 (the Agulhas Return Current) to 14 cm/s at location NP2 (the Kuroshio south of Japan), with a mean improvement of 7 cm/s. Location AG4 also shows the smallest (14%) relative improvement, while location BM1 (the Malvinas Current) shows the largest (67%) improvement. Over all locations, the mean improvement is 33%. The main reason why the (relative) improvements are not everywhere the same relates to variations in the width of the currents. Strong narrow currents are impacted more than the broader currents by the filtering required to smooth the MDTs. Because currents close to boundaries are generally narrow these in particular tend to be attenuated by filtering.

Although the currents from GOCE are a significant improvement on those from GRACE, they are still some way short, in terms of strength and definition, of those obtained from MAX09. As this latter MDT uses in-situ drifter observations of current speed to improve its short-length scales, the current speeds derived from it can be considered to be more realistic than those from the geodetic MDTs. Some of the differences between the geodetic MDTs and Maximenko MDT may be due to the different time periods to which the MDTs refer. Yet such mean period related differences are likely small in comparison with the actual differences we find. For all of the locations considered, the GOCE current speeds are less than those obtained from MAX09. In absolute terms, the differences range from a maximum of 30 cm/s at location AG2 to a minimum of 3 cm/s at locations NA3 (the Labrador Current) and NP3 (the Kuroshio Extension), with a mean difference of 12 cm/s (this compares with a mean difference of 19 cm/s for the GRACE MDT). In percentage terms, the greatest discrepancy (70%) is for location BM1 (the Brazil Current) and the smallest (3%) is for location SO1 (the Indian Ocean sector of the ACC). The mean difference is 35%, compared with 55% for the GRACE MDT. Again, the reason why GOCE comes closer to the combined MAX09 estimate for some locations than it does for others is related to the width of the currents. So we see that the greatest percentage discrepancy occurs for the Brazil Current—a narrow boundary current—while the smallest discrepancy occurs for a location on the ACC where the current is quite wide. Another good example of this is found in the North Atlantic. At the two locations considered along the Gulf Stream (NA1 and NA2) the MAX09 estimate gives a consistent estimate of about 45 cm/s. For location NA2, where the current is broader, the GOCE underestimate is 23% compared with 48% from GRACE (here GOCE is a 33% improvement upon GRACE). Yet, for location NA1, where the current is narrower and quite tightly constrained to the boundary, the GOCE underestimate is 42 and 67% for GRACE (here GOCE is a 42% improvement upon GRACE).

The main reason why the GOCE MDT is superior to that from GRACE, relates to the fact that the GOCE geoid is defined to degree and order 240 (spatial scales of roughly 83 km) while the GRACE geoid is defied only to degree and order 150 (spatial scales of roughly 133 km). Because of this, and, to a lesser extent, because the commission errors of the GOCE geoid are also smaller than those from GRACE, the GOCE MDT requires less smoothing. We found that an isotropic Gaussian filter with a half-weight radius of at least 140 km is required to remove the noise from the GOCE MDT, compared with at least 200 km for the GRACE MDT. Because less filtering is required, there is less attenuation of the MDT and associated currents. This is key to the superiority of GOCE over GRACE. But note that the difference is only 60 km. This shows the sensitivity of calculated currents to filtering and how crucial it is to filter no more than is absolutely necessary if any advantage of GOCE over GRACE is to be preserved.

Ultimately, the best solutions will come from combining geodetic observations with in-situ hydrographic and drifter data, such as done by Maximenko et al. (2009) or Rio and Hernandez (2004). However, it is still worth striving to maximize the oceanographic content of the geodetic data alone. For now, the filter radius dictates the realized resolution of

the geodetic MDTs and associated currents. However, the potential resolution is set by the degree and order of the geoid (so 83 km for the GOCE DIR solution). Fundamentally, there are two basic approaches to realizing this potential, without the introduction of auxiliary data. The first is to reduce the need to filter the MDT by reducing the noise in the unfiltered MDT. Spectral filtering of MSS to ameliorate the problem of geoid omission error can go some way towards this. But this still leaves noise due to geoid commission error. Clearly, the goal is to reduce such errors, and we can look forward to this being achieved with future GOCE gravity models based on a growing data record. However, it will be likely that some filtering will always need to be applied. This takes us to the second approach to improving the resolution of the GOCE MDTs, which is to use more sophisticated filter approaches, such as that applied by Bingham et al. (2011), which preferentially filters along MDT gradients. Theoretically, at least, it should be possible to design optimum filters based on the information contained in the GOCE full error variance–covariance matrices, which are publicly available as part of the level 2 data. In practice there are some difficulties in handling such large arrays and this is an on-going area of research.

It is worth remembering that the GOCE results presented here are based on just 2 months of observations. In spite of this, GOCE is already allowing an estimation of the ocean's geostrophic circulation that is better than any previously obtained using only satellite observations. This is a remarkable validation of the GOCE mission design and implementation. With the accumulation of many years of observations over the, now extended, lifetime of the GOCE mission we can look forward to a great advance in our ability to measure the ocean's circulation.

Acknowledgments The GOCE User Toolbox is made available by the European Space Agency through http://earth.esa.int/gut/. The analysis has been supported by the European Space Agency project "GUT2 – Version 2 of the GOCE User Toolbox", CCN 3 to ESRIN Contract No 19568/06/I-OL (4200019568). We thank the three anonymous reviewers whose comments and suggestions helped us improve the manuscript.

References

Andersen OB, Knudsen P (2009) DNSC08 mean sea surface and mean dynamic topography models. J Geophys Res 114:C11001. doi:10.1029/2008JC005179

Andersen OB, Knudsen P, Berry P (2010) The DNSC08GRA global marine gravity field from satellite altimetry. J Geod 84(3). doi:10.1007/s00190-009-0355-9

Benveniste J, Knudsen P, and the GUTS Team (2007) The GOCE user toolbox. In: Fletcher K (ed) Proceedings of the 3rd international GOCE user workshop, 6–8 November 2006, Frascati, Italy. European Space Agency, Noordwijk

Biastoch A, Böning CW, Schwarzkopf FU, Lutjeharms JRE (2009) Increase in Agulhas leakage due to poleward shift of Southern Hemisphere westerlies. Nature 462: 495–498

Bingham RJ, Haines K, Hughes CW (2008) Calculating the Ocean's mean dynamic topography from a mean sea surface and a Geoid. J Atmos Ocean Tech 25: 1808–1822. doi:10.1175/2008JTECHO568.1

Bingham RJ, Knudsen P, Andersen O, Pail R (2010) Using GOCE to estimate the mean North Atlantic circulation (Invited). Abstract G33B-08 presented at 2010 Fall Meeting, AGU, San Francisco, Calif., 13–17 Dec

Bingham RJ, Knudsen P, Andersen O, Pail R (2011) An initial estimate of the North Atlantic steady-state geostrophic circulation from GOCE. Geophys Res Lett 38:L01606. doi:10.1029/2010GL045633

Boebel O, Rae CD, Garzoli S, Lutjeharms J, Richardson P, Rossby T, Schmid C, Zenk W (1998) Float experiment studies interocean exchanges at the tip of Africa. EOS 79(1)7–8

Bruinsma S, Marty J-C, Balmino G (2004) Numerical simulation of the gravity field recovery from GOCE mission data. In: Proceedings of the second international GOCE user workshop "GOCE, The Geoid and Oceanography", 8–10 March 2004, ESA/ESRIN, Frascati, Italy (ESA SP-569, June 2004)

Bryden HL, Beal LM, Duncan LM (2005) Structure and transport of the Agulhas Current and its temporal variability. J Oceanogr 61(3):479–492

Chelton DB, Schlax MG, Witter DL, Richman JG (1990) GEOSAT altimeter observations of the surface circulation of the Southern Ocean. J Geophys Res 95: 17877–17903

Denker D, Rapp RH (1990) Geodetic and oceanographic results from the analysis of one year of geosat data. J Geophys Res 95(C8): 13151–13168

Donohue EA, Firing E, Beal L (2000) Comparison of the three velocity sections of the Agulhas current and the Agulhas undercurrent. J Geophys Res 105(C12): 28585–28593

Engelis T, Knudsen P (1989) Orbit improvement and determination of the oceanic geoid and topography from 17 days of Seasat Data. Manuscr Geod 14(3): 193–201

Förste C, Flechtner F, Schmidt R, König R, Meyer U, Stubenvoll R, Rothacher M, Barthelmes F, Neumayer H, Biancale R, Bruinsma S, Lemoine J-M, Loyer S (2006) A mean global gravity field model from the combination of satellite mission and altimetry/gravimetry surface data—EIGEN-GL04C. Geophys Res Abstr 8:03462

Friocourt Y, Drijfhout S, Blanke B, Speich S (2005) Water mass export from Drake Passage to the Atlantic, Indian, and Pacific oceans: a Lagrangian model analysis. J Phys Oceanogr 35:1206–1222

Fu L-L, Cheng B, Qiu B (2001) 25-day period large-scale oscillations in the Argentine Basin revealed by the TOPEX/POSEIDON altimeter. J Phys Oceanogr 31:506–517

Gould WJ (1985) Physical Oceanography of the Azores Front. Prog Oceanogr 14:167–190

Hogg NG, Johns WE (1995) Western boundary currents. U.S. National Report to Internatonal Union of Geodesy and Geophysics 1991–1994. Suppl Rev Geophys 33:1311–1334

Hughes CW, Bingham RJ (2008) An oceanographer's guide to GOCE and the geoid. Ocean Sci 4(1): 15–29

Johannessen JA, Balmino G, Le Provost C, Rummel R, Sabadini R, Sünkel H, Tscherning CC, Visser P, Woodworth P, Hughes CW, LeGrand P, Sneeuw N, Perosanz F, Aguirre-Martinez M, Rebhan H, Drinkwater M (2003) The European gravity field and steady-state ocean circulation explorer satellite mission: impact in geophysics. Surv Geophys 24: 339–386

Knauss JA (1996) Introduction to physical oceanography, 2nd edn. Prentice-Hall, Englewood Cliffs 152–156

Knudsen P (1991) Simultaneous estimation of the gravity field and sea surface topography from satellite altimeter data by least squares collocation. Geophys J Int 104(2): 307–317

Knudsen P (1992) Estimation of sea surface topography in the Norwegian Sea using gravimetry and geosat altimetry. Bull Géodésique 66(1):27–40

Knudsen P, Andersen OB, Forsberg R, Föh HP, Olesen AV, Vest AL, Solheim D, Omang OD, Hipkin R, Hunegnaw A, Haines K, Bingham R, Drecourt J-P, Johannessen JA, Drange H, Siegismund F, Hernandez F, Larnicol G, Rio M-H, Schaeffer P (2007) Combining altimetric/gravimetric and ocean model mean dynamic topography models in the GOCINA region. In: IAG symposia, vol 130. Springer. ISBN-10 3-540-49349-5, 3-10

Levitus S, Boyer TP (1994) World ocean atlas 1994 volume 4: temperature NOAA Atlas NESDIS 117(4). National Ocean and Atmosphere Administration USA

Manabe S, Stouffer RJ (1999) The role of thermohaline circulation in climate. Tellus Ser A 51(1): 91–109

Mann CR (1967) The termination of the Gulf Stream and the beginning of the North Atlantic Current. Deep-Sea Res 14: 337–359

Marsh JG, Koblinsky CJ, Lerch FJ, Klosko SM, Martin TV, Robbins JW, Williamson RG, Patel GB (1990) Dymanic sea surface topography, gravity, and improved orbit accuracies from the direct evaluation of Seasat altimeter data. J Geophys Res 95(C8): 13129–13150

Maximenko N, Niiler P, Rio M-H, Melnichenko O, Centurioni L, Chambers D, Zlotnicki V, Galperin B (2009) Mean dynamic topography of the ocean derived from satellite and drifting buoy data using three different techniques. J Atmos Ocean Tech 26(9):1910–1919

Nerem RS, Tapley BD, Shum CK (1990) Determination of the ocean circulation using geosat altimetry. J Geophys Res 95(C3): 3163–3179

Niiler PP, Maximenko NA, McWilliams JC (2003) Dynamically balanced absolute sea level of the global ocean derived from near-surface velocity observations. Geophys Res Lett 30(22):2164. doi:10.1029/2003GL018628

Rhines P, Hakkinen S, Josey S (2008) Is oceanic heat transport significant in the climate system?. In: Dickson RR, Meincke J, Rhines P (eds) Arctic–subarctic ocean fluxes, chap 4. Springer, New York pp 87–109

Rio M-H, Hernandez F (2004) A mean dynamic topography computed over The world ocean from altimetry, in-situ measurements and a geoid model. J Geophys Res 109(C12)

Saraceno M, Provost C, Piola AR, Bava J, Gagliardini A (2004) Brazil Malvinas Frontal System as seen from 9 years of advanced very high resolution radiometer data. J Geophys Res 109:C05027. doi:10.1029/2003JC002127

Wagner CA (1986) Accuracy estimates of geoid and ocean topography recovered jointly from satellite altimetry. J Geophys Res 91(B1): 453–461

Woodgate RA, Fahrbach E, Rohardt G (1999) Structure and transports of the East Greenland Current at 75°N from moored current meters. J Geophys Res 104(C8): 18059–18072

Wunsch C, Zlotnicki V (1984) The accuracy of altimetric surfaces. Geophys J R Astr Soc 78:795–808